

Recent tidal-flat evolution and mangrove-habitat expansion: application of radioisotope dating to environmental reconstruction

A. SWALES¹ & S. J. BENTLEY²

¹ NIWA, National Institute of Water and Atmospheric Research, PO Box 11-115, Hamilton, New Zealand
a.swales@niwa.co.nz

² Earth-Sciences Department, 6010 Alexander Murray Building, Memorial University of Newfoundland, St Johns, Newfoundland A1B 3X5, Canada

Abstract Mangrove-habitat expansion and tidal flat evolution in the Firth of Thames (North Island, New Zealand) is reconstructed using dated sediment cores (²¹⁰Pb, ¹³⁷Cs) and field observations to explore interactions between sediment processes and mangrove ecology. Mangrove habitat in the southern Firth has expanded rapidly over the last five decades, colonising prograding intertidal mudflats. The original lower-intertidal sand flat was transformed by the erosion of millions of m³ of mud following catchment deforestation (1850s–1920s). Sediment accumulation rates (SAR) on the tidal flats over the last 60 years have averaged approx. 20 mm year⁻¹, outstripping sea level rise (1.3 mm year⁻¹). Mangrove colonisation was delayed until the early 1950s when surface elevation reached approx. 0.5 m above mean sea level (MSL). Maximum SAR of approx. 100 mm year⁻¹ occurs in the seaward edge of the mangrove forest. In contrast, SAR in the landward old-growth forest have averaged <10 mm year⁻¹ since the 1970s as the forest was progressively isolated by distance and elevation from the tidal-flat. The forest today at 1.7 m above MSL is near the upper tidal limit and is infrequently inundated. Feedbacks between surface elevation, tidal inundation and sediment supply exert strong controls. The fate of the mangrove forest will depend on surface elevation increasing at a rate equal to or exceeding sea level rise.

Key words ²¹⁰Pb; ¹³⁷Cs; dating; sedimentation; surface elevation; tidal inundation; sea level

INTRODUCTION

Terrestrial sediment loads to estuaries and coasts have increased by as much as an order of magnitude or more due to human activities. In particular, deforestation and land conversion to agriculture and rapid urbanisation during the last century have accelerated soil erosion. Estuaries located on tectonically active plate margins have reached an advanced stage of infilling in many cases (Healy, 2002), due to high sediment yields from small, steep catchments subject to high rainfall (Milliman & Syvitski, 1992). This has resulted in large-scale environmental changes in estuaries, which include increased turbidity and sedimentation and a shift to increasingly mud-dominated, intertidal systems (Thrush *et al.*, 2004). Eroded terrestrial sediments have built extensive intertidal flats, which have been colonised by mangroves in temperate and tropical environments (Neil, 1998; Panapitukkul *et al.*, 1998). Mangroves enhance trapping of silts and clays by dampening currents (Furukawa *et al.*, 1997) and attenuating waves (Massel *et al.*, 1999) such that sediment accumulation rates (SAR) are highest within the fringes of mangrove forests. In this manner, mangroves influence estuarine sediment dynamics and, in doing so, the geomorphic evolution of estuaries (Thom *et al.*, 1975). Rapid mangrove-habitat expansion has occurred over recent decades in many of New Zealand's (NZ) upper North Island estuaries (Burns & Ogden, 1985; Ellis *et al.*, 2004). The grey mangrove or Manawa (*Avicennia marina* subsp. *australasica*) colonises intertidal flats down to mean sea level (MSL), where seedlings are submerged for ≤ 6 h per tide (Clarke & Myerscough, 1993). It is notable that mangrove habitat expansion in NZ estuaries has occurred half a century or more after large-scale catchment deforestation.

Short-term physical process studies are conducted in estuaries to improve understanding of mechanisms controlling sediment transport, deposition and fate. Data collected in such studies inform empirical relationships and are used to set-up and validate numerical models. However, these types of studies may not observe infrequent geomorphic events, such as storms, that drive environmental changes. Deterministic numerical models may not accurately integrate processes operating at various spatial–temporal scales and cannot generally be used to simulate long time

scales (years–millennia). To address these short-comings, complex-system models are being used to simulate the long-term behaviour and evolution of estuaries and wetlands (Kirwan *et al.*, 2008). Even so, these types of geomorphic models require quantitative data, which integrate processes operating at longer time scales. Geochronology derived from sediment-bound radioisotopes fulfils these requirements. Constant decay rates provide accurate geo-chronometers for sediments over a range of time scales. Certain radioisotopes adsorb irreversibly to clay and silt particle surfaces and are also ubiquitous in terrestrial and marine environments making them useful as tracers. Lead-210 (^{210}Pb , half-life, $t_{1/2}$, 22.3 years), a naturally occurring radioisotope, has been used to date sediments deposited in lakes, estuaries and the sea during the last approx. 150 years (Robbins & Edgington, 1975; Sharma *et al.*, 1987). Caesium-137 (^{137}Cs , $t_{1/2}$ 30 years) was first introduced to the environment by atmospheric nuclear weapons in the 1940s, although was not first detected in the southern hemisphere until the onset of large-scale weapons test in the early 1950s. ^{137}Cs provides independent and complementary dating of sediments deposited since that time.

In this paper we reconstruct the recent geomorphic evolution of a tidal flat using radioisotope dating and in doing so explore the interactions between estuarine sedimentation processes and mangrove ecology.

LOCATION

The Firth of Thames is a 800 km² meso-tidal estuarine embayment on the east-coast of the upper North Island (37°S 175.4°E) (Fig. 1). The Firth occupies a structural graben (Healy, 2002), which is bounded to the east and west by the Coromandel Peninsula and Hunua Ranges, respectively. The Firth receives freshwater runoff from a 3600 km² catchment, with the largest sediment inputs from the Waihou (1966 km²) and Piako (1476 km²) sub-catchments. Large-scale deforestation of the Coromandel ranges, associated with logging and gold-mining, followed the arrival of European settlers from the mid-1800s onwards (Brownell, 2004). Mud supplied by catchment soil erosion has built approx. 70 km² of intertidal mudflats along the southern shore of the Firth (Fig. 1).

Tides in the Firth are semi-diurnal, with average spring- and neap-tidal ranges of 2.9-m and 2.2-m, respectively. Tidal-current speeds are $\leq 0.3 \text{ m s}^{-1}$ on an average tide. Estuarine circulation and prevailing southwest and northeast winds that drive residual circulation trap river-borne suspended sediments within the Firth (Healy, 2002). Northerly winds generate short-period ($T < 6 \text{ s}$) waves typically $< 1 \text{ m}$ high (Woodroffe *et al.*, 1983). Tidal-flat morphology is similar to that described for the Surinam coast of South America (Wells and Colman, 1981). The lower-intertidal

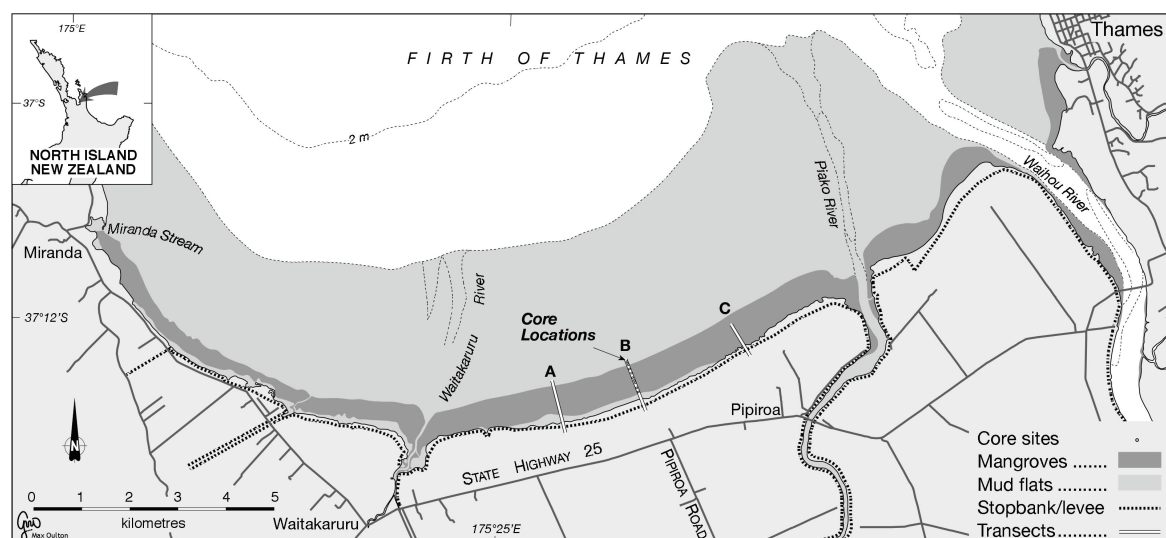


Fig. 1 Location of the study area, southern Firth of Thames, New Zealand.

flat is characterized by fluid mud, while isolated mud mounds ≤ 20 cm high occur on the middle–upper intertidal flat. The upper tidal flat immediately seaward of the mangrove forest is occupied by a 300-m wide zone of large-scale “mud forms”. These shore-normal bed features are ≤ 0.25 m high with wavelengths ≤ 2 m and resemble an irregular ridge-runnel system. This morphology is characteristic of mesotidal, moderately wave-exposed, mud flats, with large mud supply and rapid sedimentation (Mehta, 2002). Rapid mangrove-habitat expansion in the southern Firth is a relatively recent phenomenon. Captain Cook visited the Firth in 1769 and noted mangrove stands along the lower Waihou River (Brownell, 2004) and mangrove stands were still restricted to river deltas as recently as the early 1950s. Today, mangrove forest extends 1 km seaward of the 1952 shoreline and occupies approx. 11 km² of former tidal flat.

METHODS

Sediment cores

Sediment cores up to 2 m long were collected at 10 sites (C3 to C12) along a 700-m shore-normal transect through the mangrove forest to the present-day tidal flat (Fig. 1). Cores were extracted using a 7.5-cm-diameter piston corer, with core compression being $< 5\%$. X-radiographs of 2-cm thick longitudinal slabs taken from the cores were used to study sedimentary structures such as bedding and animal burrows. These data informed the interpretation of the radioisotope profiles. The cores were sub-sampled at intervals down core for radioisotope, dry bulk density and particle-size analysis. Bulk density data were used to estimate radioisotope inventories in each core. Particle-size was determined using a time-of-transition, stream-scanning-laser particle sizer.

Sediment accumulation rates

Sediment accumulation rates (SAR) were estimated by ²¹⁰Pb and ¹³⁷Cs dating. Radioisotope activity concentrations (hereafter concentrations) expressed in S.I. units of Becquerel (disintegration s⁻¹) per kilogram (Bq kg⁻¹) were determined by gamma spectrometric analysis of dried sediment. The unsupported or excess ²¹⁰Pb (²¹⁰Pb_{ex}) was determined from the ²²⁶Ra (*t*_{1/2} 1622 years) assay after a 30-d ingrowth period for ²²²Rn (*t*_{1/2} 3.8 days). Time-averaged SAR (mm year⁻¹) were calculated from the vertical ²¹⁰Pb_{ex} profiles in each core, assuming that no physical or biological mixing of the sediment column occurred below the depth of the surface mixed layer (SML). If sediment accumulation is the dominant process and steady-state conditions are assumed (Nittrouer & Sternberg, 1981), mixing can be ignored and the accumulation rate (*S*, mm year⁻¹) can be estimated from the least-squares fit to the ²¹⁰Pb_{ex} profile:

$$A_z = A_0 \exp(-\lambda z/S) \quad (1)$$

where λ is the decay constant for ²¹⁰Pb (0.031⁻¹ year), *S* is the sedimentation rate, *A* is the unsupported ²¹⁰Pb activity at depth *z*. The apparent age of sediment at a particular depth is thus an exponential function of the initial surface activity of ²¹⁰Pb_{ex} (*A*₀), λ and *S*. The ²¹⁰Pb_{ex} concentration factor was estimated for each core from the ratio of the mean annual atmospheric supply rate (*P*, Bq cm⁻² year⁻¹) and the measured ²¹⁰Pb atmospheric flux (*P*_{atm}, 0.005 Bq cm⁻² year⁻¹, NIWA unpublished data). The mean ²¹⁰Pb_{ex} supply rate is given by *P* = *kI*, where *I* is the total ²¹⁰Pb_{ex} inventory (Bq cm⁻²) in each core estimated from the least-squares fit to the ²¹⁰Pb_{ex} profile.

SAR were also estimated from the maximum penetration depth of ¹³⁷Cs profiles in the sediment column. In New Zealand, deposition of ¹³⁷Cs from the atmosphere was first detected in 1953, with peak deposition occurring in 1963–1964. For ¹³⁷Cs dating, we assumed that: (a) ¹³⁷Cs introduced in 1953 and rapidly transferred to depositing sediments and was rapidly mixed in the SML; and (b) core compaction is minimal, such that *S* can be calculated from:

$$S = (z_p - z_b)/t_0 - t_i \quad (2)$$

where *z*_p is the maximum penetration depth of ¹³⁷Cs, *z*_b is the depth of the SML, *t*₀ is the year sediment cores were collected and *t*_i is the year ¹³⁷Cs was introduced to the environment (1953).

Mangrove-habitat expansion

The historical sequence of mangrove-habitat expansion in the southern Firth of Thames was reconstructed from the aerial photographic record (1944–2006). These images were digitised and mosaics geo-referenced to ground control points using Intergraph Geomedia GIS software.

Tidal-flat morphology

The large-scale morphology of the tidal flat was determined from three shore-normal elevation transects (A–C) located at approx. 2-km intervals alongshore (Fig. 1). The transects extended ≤ 1200 -m seaward from the stopbank, through the mangrove forest to the intertidal flat. Surface elevations were measured to ± 0.5 cm accuracy using a total station and reduced to mean sea level (MSL) Moturiki Vertical Datum 1953. The frequency and duration of tidal inundation of the mangrove forest was determined using a local sea-level record (Swales *et al.*, 2007). The recent evolution of the tidal flat was reconstructed from the radioisotope geochronology, present-day surface elevations and historical aerial photography. An age–surface elevation (ASE) curve was constructed for the tidal flat that has developed under the mangrove forest over the last 60 years. Past surface elevations for years coinciding with the aerial photographs were estimated at each core site from the present-day surface elevation and ^{210}Pb SAR. To do this, we assumed that sediment compaction has been negligible, which was consistent with high water content and SAR observed in the cores. Historical tidal-flat surface elevations were averaged for sets of cores coinciding with various phases of the mangrove forest development.

RESULTS AND DISCUSSION

Mangrove-habitat expansion

The historical aerial photographs indicate at least four major mangrove-seedling recruitment events have occurred in the southern Firth since the early-1950s (Swales *et al.*, 2007). We distinguish between the old-growth mangrove forest that first colonized the mudflats in the early 1950s and recent mangrove forest that has developed since the mid 1980s. The boundary between these old and recent forests occurs near site C6 (Fig. 2(b)). Forest classification is based on the aerial photographs which indicate large-scale forest loss sometime during the period 1977–1987. The pattern and scale of destruction is indicative of storm damage, of sufficient magnitude to

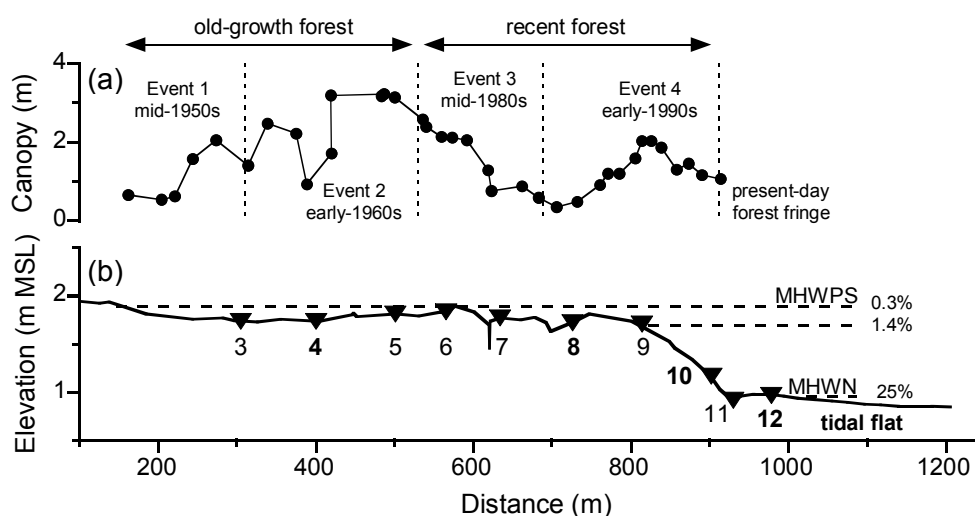


Fig. 2 Transect B: (a) mangrove forest average canopy height, with timing of major seedling recruitment events indicated; (b) surface elevation relative to mean sea level (MSL), duration of tidal inundation (% of total time) and core locations (C3–C12).

destroy several hectares of the mangrove forest mainly along its seaward fringe (Swales *et al.*, 2007). Variations in forest-canopy height along Transect B reflect each phase of mangrove-habitat expansion, with a repeating pattern of taller trees immediately seaward of dwarf stands (Fig. 2(a)). Stands of taller trees occur at historical as well as the present-day position of the seaward fringe of the forest. Mangroves first colonised the tidal flat close to C3 at Transect B and approx. 300-m seaward of the 1952 shoreline. By 1977, mangrove forest occupied a continuous 500-m wide zone on the middle–upper tidal flat. Further forest expansion occurred in the mid 1980s and 1990s, although no major seedling recruitment events have occurred in the last decade. Today, some 740 hectares of mangrove forest occupy former tidal flats.

Observations of seedling recruitment on the tidal flat near the forest fringe show that mortality of mangrove propagules is primarily controlled by episodic wave-driven erosion of the substrate in which the seedlings are rooted (Swales *et al.*, 2007), as observed in southern Australia (Clarke & Myerscough, 1991). Swales *et al.* (2007) concluded that successful seedling recruitment in the summer coincides with infrequent, extended periods of calm weather, which occur on average once per decade. These observations along with the aerial photographs and forest structure data indicate that major seedling recruitment events and thus mangrove habitat expansion are controlled by wind climate.

Present-day morphology

The present-day tidal flat has a convex-upward profile that is characteristic of stable or prograding muddy-coasts (Fig. 2(b), Mehta, 2002). Surface elevation in the mangrove forest at 1.7–1.9 m above MSL is close to the upper limit of the tide at mean high water perigean spring tide (MHWPS) level at 1.87 m above MSL, which is inundated $\leq 0.3\%$ of the time. The creek drainage network is poorly developed due to the small tidal prism and infrequency of inundation. Surface elevation declines in the forest fringe (i.e. seaward of C9) from 1.7 to 1 m above MSL at the seaward edge of the forest. This coincides with mean high water neap (MHWN) tide elevation, where the tidal flat is inundated 25% of the time. Thus, the mangrove forest is infrequently inundated during the fortnightly spring–neap tidal cycle (Fig. 2(b)).

Mangrove-forest sedimentation

The radioisotope profiles measured in the sediment cores indicate substantial differences in the sedimentation chronologies between the old-growth and recent mangrove forests. The radioisotope record at site C4 is representative of the sedimentation history of the old-growth mangrove forest (Fig. 3). Mangroves first colonised the tidal flat at this site in the mid 1960s. Sediments here consist of a homogenous low density mud ($\text{DBD} = 0.5 \text{ g cm}^{-3}$), with a median particle diameter of 7–16 μm (Fig. 3). The $^{210}\text{Pb}_{\text{ex}}$ profile extends to 1.8 m depth and has a characteristic stair-step form (Fig. 3(c)). This type of profile indicates abrupt changes in SAR between periods of relatively constant sedimentation. ^{210}Pb dating shows that basal sediments below 1.2 m depth were deposited before the mid-1960s and as early as the 1930s. This is consistent with the presence of ^{137}Cs to 1.5 m depth, which labels sediments deposited since the early 1950s. A notable feature of the ^{137}Cs profile is the absence of concentration maxima coinciding with atmospheric ^{137}Cs deposition peaks in the 1950s and 1960s that have been observed in lake sediments (Robbins & Edgington, 1975). The homogeneous ^{137}Cs concentrations at Site C4 reflect the variety of ^{137}Cs sources, (i.e. direct atmospheric deposition, tidal flat and eroded soil), transport and mixing before final deposition. This early period coincides with the rapid accretion of the tidal flat (22 mm year^{-1}) and is similar to SAR measured on the unvegetated tidal flat today (Swales *et al.*, 2007). The onset of mangrove colonisation and tree growth on the forest fringe at Site C4 during the mid-1960s is indicated by a five-fold increase in SAR to 100 mm year^{-1} . Some 0.8 m of mud was deposited during the approx. 8 years that the forest fringe occupied this site. The subsequent seaward expansion of the mangrove forest in the early 1970s isolated the site from the tidal flat, with a resulting decline in the $^{210}\text{Pb}_{\text{ex}}$ SAR to 12 mm year^{-1} . This pattern of increasing sedimentation during mangrove

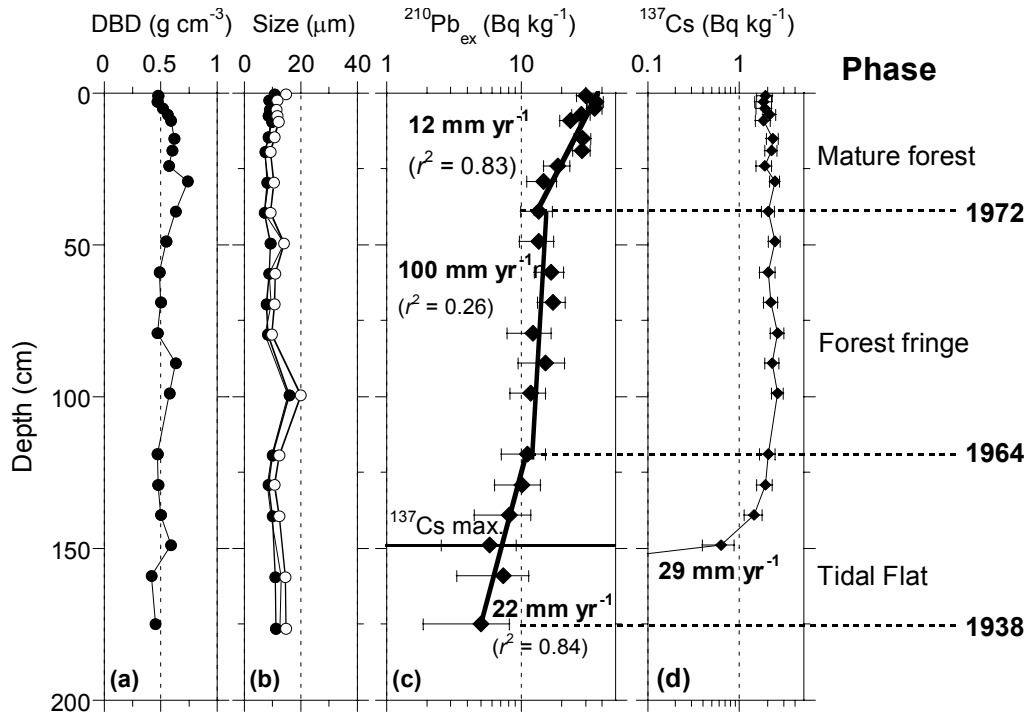


Fig. 3 Old-growth forest (Core C4) sediment profiles: (a) dry bulk sediment density (DBD); (b) particle size statistics, median (open symbol) and mean (closed symbol) diameters and standard deviation (line); (c) unsupported $^{210}\text{Pb}_{\text{ex}}$ concentration with 95% confidence intervals shown. Time-averaged sediment accumulation rates (SAR) and co-efficient of determination (r^2) derived from fit to the data; (d) ^{137}Cs concentration profile and SAR.

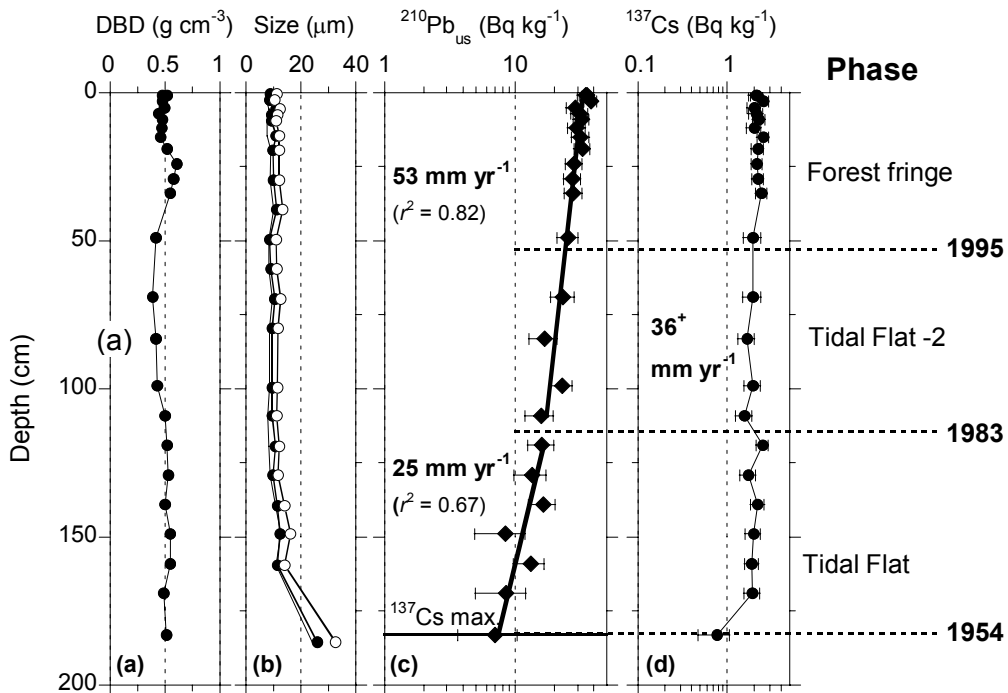


Fig. 4 Recent forest (Core C8) sediment profiles: (a) dry bulk sediment density (DBD); (b) particle size statistics, median (open symbol) and mean (closed symbol) diameters and standard deviation (line); (c) unsupported $^{210}\text{Pb}_{\text{us}}$ concentration with 95% confidence intervals shown. Time-averaged sediment accumulation rates (SAR) and co-efficient of determination (r^2) derived from fit to the data; (d) ^{137}Cs concentration profile and SAR.

colonisation and subsequent decline is consistent with the progressive seaward advance of mangrove habitat on the tidal flat.

Core C8 records the accelerated sedimentation of the tidal flat and the most recent phase of mangrove habitat expansion that occurred in the mid-1990s (Fig. 4).

The sediment profiles show that the low density muds, characteristic of deposits in the mangrove forest, are replaced by laminated silts and sands below 100-cm depth (Fig. 4(a),(b)) at 0.2 m above MSL. These deposits are characteristic of energetic tidal-flat environments (Reineck & Singh, 1980). The ^{210}Pb dating of basal sediments to the early 1950s is in close agreement with the maximum depth of ^{137}Cs . Unlike the old-growth forest, mangrove colonisation was preceded by an increase in SAR from 25 mm to 53 mm year⁻¹ in the previous decade. Site C8 coincides with the dwarf mangrove, immediately behind the tallest trees on the present-day fringe (Site C9), where SAR have exceeded 100 mm year⁻¹.

The $^{210}\text{Pb}_{\text{ex}}$ mean supply rates estimated from the core inventories (0.0038–0.117 Bq cm⁻² year⁻¹) are 6–20 times higher than predicted by the direct ^{210}Pb atmospheric flux (0.005 Bq cm⁻² year⁻¹). This large $^{210}\text{Pb}_{\text{ex}}$ surplus reflects the import of ^{210}Pb associated with sedimentation over the last 50 years and indicates that the mangrove forest is a long-term sink for fine sediments delivered to the Firth.

Tidal-flat evolution and mangrove-forest fate

The long-term fate of mangrove forests depends on surface elevation increasing at a rate equal to or exceeding sea level rise (McKee *et al.*, 2007). In the context of the present study, mangrove forest SAR over the last approx. 60 years have been orders of magnitude higher than the average relative rate of sea level rise (SLR) since the late 1800s (1.3 mm year⁻¹, Hannah, 2004) and average SAR of <5 mm year⁻¹ in most North Island estuaries.

Tidal-flat evolution over the last 60 years is reconstructed from the age–surface elevation (ASE) curve for the old-growth mangrove forest (Fig. 5). The ASE curve identifies the temporal pattern of surface elevation change that is not readily apparent from the radioisotope profiles. The rate of surface elevation change increased as the tidal flat was first colonised by mangroves in the early 1950s, and increased on average by 65 mm year⁻¹ as mud was rapidly deposited in a forest fringe environment.

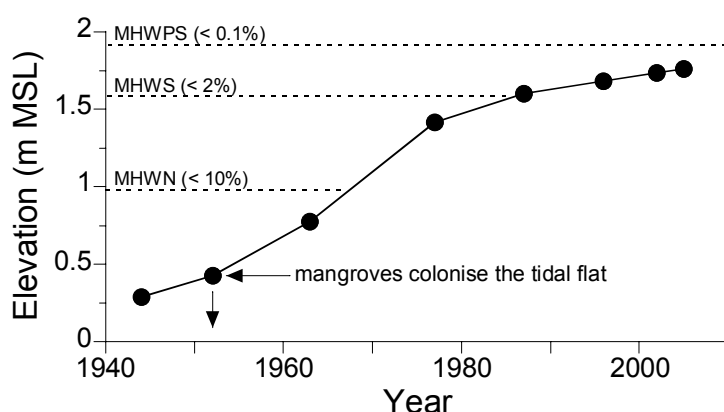


Fig. 5 Age–surface elevation curve for the old-growth mangrove forest (C3–C5). Also shown are high-tide elevations relative to mean sea level (MSL) Moturiki Vertical Datum 1953. The surface elevation data coincide with the aerial photographic record.

The rate of surface elevation change declined to <9 mm year⁻¹ from the late 1970s as mangrove colonised the tidal flat further seaward and the old-growth forest was progressively isolated by distance and elevation from the tidal-flat mud supply. By 1990, the average surface

elevation reached MHWS and today the old-growth forest is infrequently flooded during high spring and storm tides (Swales *et al.*, 2007). This pattern of initial rapid increase in surface elevation, followed by a transition to more modest elevation changes is also observed in salt-marsh systems. This asymptotic behaviour reflects a progressive reduction in the frequency and duration of tidal inundation and sediment supply (Allen, 1990). Today, average surface elevation in the mangrove forest is close to the upper limit of the tide so that SAR are likely to be approaching the relative SLR rate. Global warming is predicted to increase average eustatic SLR rates to 5–8 mm year⁻¹ by 2100 AD (Solomon *et al.*, 2007). In the Caribbean, mangrove forests have accommodated eustatic SLR rates of up to 4 mm year⁻¹ during the Holocene by peat deposition (Mc Kee *et al.*, 2007). By contrast, NZ mangrove systems have accumulated eroded terrestrial fine sediments. There is uncertainty about how NZ mangrove forests will respond to climate changes that are likely to influence mangrove growth, catchment sediment yields, wave climate and storm-tide frequency, which are key drivers of mangrove-habitat expansion.

Acknowledgements This research was funded by Environment Waikato (EW) and the NZ Foundation of Research, Science and Technology (Contract CO1X0307). We thank EW staff for GIS analysis of the historical aerial photographs. Ron Ovenden, Cliff Hart and Mark Smith (NIWA) assisted with field work. Dr Catherine Lovelock (Centre for Marine Studies, University of Queensland) provided canopy-height data. We thank Dr Mark Pritchard (NIWA) for constructive comments on a draft of this paper.

REFERENCES

- Allen, J. R. L. (1990) Salt-marsh growth and stratification: A numerical model with special reference to the Severn Estuary, southwest Britain. *Marine Geol.* **95**, 77–96.
- Brownell, B. (2004) *Muddy feet: Firth of Thames RAMSAR-site update 2004*. Ecoquest Education Foundation, Pokeno, New Zealand.
- Burns, B. R. & Ogden, J. (1985) The demography of the temperate mangrove (*Avicennia marina* (Forsk.) Vierh.) at its southern limit in New Zealand. *Australian J. Ecol.* **10**, 125–133.
- Clarke, P. J. & Myerscough, P. J. (1993) The intertidal distribution of the grey mangrove (*Avicennia marina*) in southeastern Australia: the effects of physical conditions, interspecific competition, and predation on propagule establishment and survival. *Australian J. Ecol.* **18**, 307–315.
- Ellis, J, Nicholls, P., Craggs, R., Hofstra, D. & Hewitt, J. (2004) Effects of terrigenous sedimentation on mangrove physiology and associated macrobenthic communities *Marine Ecology Progress Series* **270**, 71–82.
- Furukawa, K., Wolanski, E. & Mueller, H. (1997) Currents and sediment transport in mangrove forests. *Estuarine, Coastal and Shelf Science* **44**, 301–310.
- Hannah, J. (2004) An updated analysis of long-term sea level change in New Zealand. *Geophys. Res. Lett.* **31**(L03307), 1–4.
- Healy, T. (2002) Muddy coasts of mid-latitude oceanic islands on an active plate margin, New Zealand. In: *Muddy Coasts of the World: Processes, Deposits and Function* (ed. by T. Healy & J.-A. Yang), 347–374. Cambridge University Press, Cambridge, UK.
- Kirwan, M. L., Murray, A. B. & Boyd, S. (2008) Temporary vegetation disturbances as an explanation for permanent loss of tidal wetlands. *Geophys. Res. Lett.* **35**, L05403, doi: 10.1029/2007GL032681.
- Massel, S. R., Furukawa, K. & Brinkman, R. M. (1999) Surface wave propagation in mangrove forests. *Fluid Dynamics Res.* **24**, 219–249.
- McKee, K. L., Cahoon, D. R. & Feller, I. C. (2007) Caribbean mangroves adjust to rising sea level through biotic controls on change in soil elevation. *Global Ecology Biogeography* doi: 10.1111/j.1466-8238.2007.00317.x.
- Mehta, A. J. (2002) Mud-shore dynamics and controls. In: *Muddy Coasts of the World: Processes, Deposits and Function* (ed. by T. Healy & J.-A. Yang), 19–60. Cambridge University Press, Cambridge, UK.
- Milliman, J. D. & Syvitski, J. P. M. (1992) Geomorphic/tectonic control of sediment discharge to the ocean: the importance of small mountainous rivers. *J. Geol.* **100**, 525–544.
- Neil, D.T. (1998) Moreton Bay and its catchment: seascape and landscape, development and degradation. In: *Moreton Bay and Catchment* (ed. by I. R. Tibbetts, N. J. Hall & W. C. Dennison), 3–54. University of Queensland, Australia.
- Nittrouer, C. A. & Sternberg, R. W. (1981) The formation of sedimentary strat in an allocthonous shelf environment: The Washington continental shelf. *Marine Geol.* **42**, 201–232.
- Panapitukkul, N., Duarte, C. M., Thampanya, U., Kheowvongsri, P., Srichai, O., Geertz-Hansen, Terrados, J. & Boromthananarath, S. (1998) Mangrove colonisation: mangrove progression over the growing Pak Phanang (SE Thailand) mud flat. *Estuarine, Coastal and Shelf Science* **47**, 51–61.
- Reineck, H. E. & Singh, I. B. (1980) *Depositional Sedimentary Environments*, second revised edition. Springer-Verlag, Berlin, Germany.
- Robbins, J. A. & Edgington, D. N. (1975) Determination of recent sedimentation rates in Lake Michigan using ²¹⁰Pb and ¹³⁷Cs. *Geochimica et Cosmochimica Acta* **39**, 285–304.

- Sharma, K., Gardner, L. R., Moore, W. S. & Bollinger, M. S. (1987) Sedimentation and bioturbation in a saltmarsh revealed by ^{210}Pb , ^{137}Cs and ^7Be studies. *Limnology & Oceanography* **32**(2), 313–326.
- Solomon, S., Qin, D., Manning, M., Chen, Z., Marquis, M., Averyt, K. B., Tignor, M. & Miller, H. L. (2007) *Climate Change 2007: The Physical Science Basis*. Contribution of Working Group I to the fourth assessment report of the Intergovernmental Panel on Climate Change. Cambridge University Press, Cambridge, UK.
- Swales, A., Bentley, S. J., Lovelock, C. & Bell, R. G. (2007) Sediment processes and mangrove-habitat expansion on a rapidly prograding muddy coast, New Zealand. In: *Coastal Sediments 2007* (ed. by N. C. Krauss & J. D. Rosati), 1441–1454. (Proceedings of the Sixth International Symposium on Coastal Engineering and Science of Coastal Sediment Processes) ACSE, Reston, Virginia, USA.
- Thom, B. G., Wright, L. D. & Coleman, J.M. (1975) Mangrove ecology and deltaic geomorphology: Cambridge–Ord River, Western Australia. *J. Ecol.* **63**, 203–232.
- Thrush, S. F., Hewitt, J. E., Cummings, V. J., Ellis, J. I., Hatton, C., Lohrer, A. & Norkko, A. (2004) Muddy waters: elevating sediment input to coastal and estuarine habitats. *Frontiers in Ecology and the Environment* **2**(6), 299–306.
- Wells, J. T. & Coleman, J. M. (1981) Physical processes and fine-grained sediment dynamics, coast of Surinam, South America. *J. Sedimentary Petrology* **51**, 1053–1068.
- Woodroffe, C. D., Curtis, R. J. & McLean, R. F. (1983) Development of a chenier plain, Firth of Thames, New Zealand. *Marine Geol.* **53**, 1–22.